

Beam energy dependence of charge separation along the magnetic field in Au+Au collisions at RHIC

L. Adamczyk,¹ J. K. Adkins,²³ G. Agakishiev,²¹ M. M. Aggarwal,³⁵ Z. Ahammed,⁵³ I. Alekseev,¹⁹ J. Alford,²² C. D. Anson,³² A. Aparin,²¹ D. Arkhipkin,⁴ E. C. Aschenauer,⁴ G. S. Averichev,²¹ A. Banerjee,⁵³ D. R. Beavis,⁴ R. Bellwied,⁴⁹ A. Bhasin,²⁰ A. K. Bhati,³⁵ P. Bhattarai,⁴⁸ H. Bichsel,⁵⁵ J. Bielcik,¹³ J. Bielcikova,¹⁴ L. C. Bland,⁴ I. G. Bordyuzhin,¹⁹ W. Borowski,⁴⁵ J. Bouchet,²² A. V. Brandin,³⁰ S. G. Brovko,⁶ S. Bültmann,³³ I. Bunzarov,²¹ T. P. Burton,⁴ J. Butterworth,⁴¹ H. Caines,⁵⁷ M. Calderón de la Barca Sánchez,⁶ D. Cebra,⁶ R. Cendejas,³⁶ M. C. Cervantes,⁴⁷ P. Chaloupka,¹³ Z. Chang,⁴⁷ S. Chattopadhyay,⁵³ H. F. Chen,⁴² J. H. Chen,⁴⁴ L. Chen,⁹ J. Cheng,⁵⁰ M. Cherney,¹² A. Chikanian,⁵⁷ W. Christie,⁴ J. Chwastowski,¹¹ M. J. M. Codrington,⁴⁸ G. Contin,²⁶ J. G. Cramer,⁵⁵ H. J. Crawford,⁵ X. Cui,⁴² S. Das,¹⁶ A. Davila Leyva,⁴⁸ L. C. De Silva,¹² R. R. Debbé,⁴ T. G. Dedovich,²¹ J. Deng,⁴³ A. A. Derevschikov,³⁷ R. Derradi de Souza,⁸ S. Dhamija,¹⁸ B. di Ruzza,⁴ L. Didenko,⁴ C. Dilks,³⁶ F. Ding,⁶ P. Djawotho,⁴⁷ X. Dong,²⁶ J. L. Drachenberg,⁵² J. E. Draper,⁶ C. M. Du,²⁵ L. E. Dunkelberger,⁷ J. C. Dunlop,⁴ L. G. Efimov,²¹ J. Engelage,⁵ K. S. Engle,⁵¹ G. Eppley,⁴¹ L. Eun,²⁶ O. Evdokimov,¹⁰ O. Eyser,⁴ R. Fatemi,²³ S. Fazio,⁴ J. Fedorisin,²¹ P. Filip,²¹ E. Finch,⁵⁷ Y. Fisyak,⁴ C. E. Flores,⁶ C. A. Gagliardi,⁴⁷ D. R. Gangadharan,³² D. Garand,³⁸ F. Geurts,⁴¹ A. Gibson,⁵² M. Girard,⁵⁴ S. Gliske,² L. Greiner,²⁶ D. Grosnick,⁵² D. S. Gunarathne,⁴⁶ Y. Guo,⁴² A. Gupta,²⁰ S. Gupta,²⁰ W. Guryn,⁴ B. Haag,⁶ A. Hamed,⁴⁷ L.-X. Han,⁴⁴ R. Haque,³¹ J. W. Harris,⁵⁷ S. Heppelmann,³⁶ A. Hirsch,³⁸ G. W. Hoffmann,⁴⁸ D. J. Hofman,¹⁰ S. Horvat,⁵⁷ B. Huang,⁴ H. Z. Huang,⁷ X. Huang,⁵⁰ P. Huck,⁹ T. J. Humanic,³² G. Igo,⁷ W. W. Jacobs,¹⁸ H. Jang,²⁴ E. G. Judd,⁵ S. Kabana,⁴⁵ D. Kalinkin,¹⁹ K. Kang,⁵⁰ K. Kauder,¹⁰ H. W. Ke,⁴ D. Keane,²² A. Kechechyan,²¹ A. Kesich,⁶ Z. H. Khan,¹⁰ D. P. Kikola,⁵⁴ I. Kisel,¹⁵ A. Kisiel,⁵⁴ D. D. Koetke,⁵² T. Kollegger,¹⁵ J. Konzer,³⁸ I. Koralt,³³ L. Kotchenda,³⁰ A. F. Kraishan,⁴⁶ P. Kravtsov,³⁰ K. Krueger,² I. Kulakov,¹⁵ L. Kumar,³¹ R. A. Kycia,¹¹ M. A. C. Lamont,⁴ J. M. Landgraf,⁴ K. D. Landry,⁷ J. Lauret,⁴ A. Lebedev,⁴ R. Lednický,²¹ J. H. Lee,⁴ M. J. LeVine,⁴ C. Li,⁴² W. Li,⁴⁴ X. Li,³⁸ X. Li,⁴⁶ Y. Li,⁵⁰ Z. M. Li,⁹ M. A. Lisa,³² F. Liu,⁹ T. Ljubicic,⁴ W. J. Llope,⁴¹ M. Lomnitz,²² R. S. Longacre,⁴ X. Luo,⁹ G. L. Ma,⁴⁴ Y. G. Ma,⁴⁴ D. M. M. D. Madagadgettige Don,¹² D. P. Mahapatra,¹⁶ R. Majka,⁵⁷ S. Margetis,²² C. Markert,⁴⁸ H. Masui,²⁶ H. S. Matis,²⁶ D. McDonald,⁴⁹ T. S. McShane,¹² N. G. Minaev,³⁷ S. Mioduszewski,⁴⁷ B. Mohanty,³¹ M. M. Mondal,⁴⁷ D. A. Morozov,³⁷ M. K. Mustafa,²⁶ B. K. Nandi,¹⁷ Md. Nasim,³¹ T. K. Nayak,⁵³ J. M. Nelson,³ G. Nigmatkulov,³⁰ L. V. Nogach,³⁷ S. Y. Noh,²⁴ J. Novak,²⁹ S. B. Nurushev,³⁷ G. Odyniec,²⁶ A. Ogawa,⁴ K. Oh,³⁹ A. Ohlson,⁵⁷ V. Okorokov,³⁰ E. W. Oldag,⁴⁸ D. L. Olvitt Jr.,⁴⁶ M. Pachr,¹³ B. S. Page,¹⁸ S. K. Pal,⁵³ Y. X. Pan,⁷ Y. Pandit,¹⁰ Y. Panebratsev,²¹ T. Pawlak,⁵⁴ B. Pawlik,³⁴ H. Pei,⁹ C. Perkins,⁵ W. Peryt,⁵⁴ P. Pile,⁴ M. Planinic,⁵⁸ J. Pluta,⁵⁴ N. Poljak,⁵⁸ J. Porter,²⁶ A. M. Poskanzer,²⁶ N. K. Pruthi,³⁵ M. Przybycien,¹ P. R. Pujahari,¹⁷ J. Putschke,⁵⁶ H. Qiu,²⁶ A. Quintero,²² S. Ramachandran,²³ R. Raniwala,⁴⁰ S. Raniwala,⁴⁰ R. L. Ray,⁴⁸ C. K. Riley,⁵⁷ H. G. Ritter,²⁶ J. B. Roberts,⁴¹ O. V. Rogachevskiy,²¹ J. L. Romero,⁶ J. F. Ross,¹² A. Roy,⁵³ L. Ruan,⁴ J. Rusnak,¹⁴ O. Rusnakova,¹³ N. R. Sahoo,⁴⁷ P. K. Sahu,¹⁶ I. Sakrejda,²⁶ S. Salur,²⁶ J. Sandweiss,⁵⁷ E. Sangaline,⁶ A. Sarkar,¹⁷ J. Schambach,⁴⁸ R. P. Scharenberg,³⁸ A. M. Schmah,²⁶ W. B. Schmidke,⁴ N. Schmitz,²⁸ J. Seger,¹² P. Seyboth,²⁸ N. Shah,⁷ E. Shahaliev,²¹ P. V. Shanmuganathan,²² M. Shao,⁴² B. Sharma,³⁵ W. Q. Shen,⁴⁴ S. S. Shi,²⁶ Q. Y. Shou,⁴⁴ E. P. Sichtermann,²⁶ R. N. Singaraju,⁵³ M. J. Skoby,¹⁸ D. Smirnov,⁴ N. Smirnov,⁵⁷ D. Solanki,⁴⁰ P. Sorensen,⁴ H. M. Spinka,² B. Srivastava,³⁸ T. D. S. Stanislaus,⁵² J. R. Stevens,²⁷ R. Stock,¹⁵ M. Strikhanov,³⁰ B. Stringfellow,³⁸ M. Sumner,¹⁴ X. Sun,²⁶ X. M. Sun,²⁶ Y. Sun,⁴² Z. Sun,²⁵ B. Surrøw,⁴⁶ D. N. Svirida,¹⁹ T. J. M. Symons,²⁶ M. A. Szelezniak,²⁶ J. Takahashi,⁸ A. H. Tang,⁴ Z. Tang,⁴² T. Tarnowsky,²⁹ J. H. Thomas,²⁶ A. R. Timmins,⁴⁹ D. Tlusty,¹⁴ M. Tokarev,²¹ S. Trentalange,⁷ R. E. Tribble,⁴⁷ P. Tribedy,⁵³ B. A. Trzeciak,¹³ O. D. Tsai,⁷ J. Turnau,³⁴ T. Ullrich,⁴ D. G. Underwood,² G. Van Buren,⁴ G. van Nieuwenhuizen,²⁷ M. Vandenbroucke,⁴⁶ J. A. Vanfossen, Jr.,²² R. Varma,¹⁷ G. M. S. Vasconcelos,⁸ A. N. Vasiliev,³⁷ R. Vertesi,¹⁴ F. Videbæk,⁴ Y. P. Vijoyi,⁵³ S. Vokal,²¹ A. Vossen,¹⁸ M. Wada,⁴⁸ F. Wang,³⁸ G. Wang,⁷ H. Wang,⁴ J. S. Wang,²⁵ X. L. Wang,⁴² Y. Wang,⁵⁰ Y. Wang,¹⁰ G. Webb,²³ J. C. Webb,⁴ G. D. Westfall,²⁹ H. Wieman,²⁶ S. W. Wissink,¹⁸ R. Witt,⁵¹ Y. F. Wu,⁹ Z. Xiao,⁵⁰ W. Xie,³⁸ K. Xin,⁴¹ H. Xu,²⁵ J. Xu,⁹ N. Xu,²⁶ Q. H. Xu,⁴³ Y. Xu,⁴² Z. Xu,⁴ W. Yan,⁵⁰ C. Yang,⁴² Y. Yang,²⁵ Y. Yang,⁹ Z. Ye,¹⁰ P. Yepes,⁴¹ L. Yi,³⁸ K. Yip,⁴ I.-K. Yoo,³⁹ N. Yu,⁹ Y. Zawisza,⁴² H. Zbroszczyk,⁵⁴ W. Zha,⁴² J. B. Zhang,⁹ J. L. Zhang,⁴³ S. Zhang,⁴⁴ X. P. Zhang,⁵⁰ Y. Zhang,⁴² Z. P. Zhang,⁴² F. Zhao,⁷ J. Zhao,⁹ C. Zhong,⁴⁴ X. Zhu,⁵⁰ Y. H. Zhu,⁴⁴ Y. Zoukarneeva,²¹ and M. Zyzak¹⁵

(STAR Collaboration)

- ¹AGH University of Science and Technology, Cracow, Poland
²Argonne National Laboratory, Argonne, Illinois 60439, USA
³University of Birmingham, Birmingham, United Kingdom
⁴Brookhaven National Laboratory, Upton, New York 11973, USA
⁵University of California, Berkeley, California 94720, USA
⁶University of California, Davis, California 95616, USA
⁷University of California, Los Angeles, California 90095, USA
⁸Universidade Estadual de Campinas, Sao Paulo, Brazil
⁹Central China Normal University (HZNU), Wuhan 430079, China
¹⁰University of Illinois at Chicago, Chicago, Illinois 60607, USA
¹¹Cracow University of Technology, Cracow, Poland
¹²Creighton University, Omaha, Nebraska 68178, USA
¹³Czech Technical University in Prague, FNSPE, Prague, 115 19, Czech Republic
¹⁴Nuclear Physics Institute AS CR, 250 68 Řež/Prague, Czech Republic
¹⁵Frankfurt Institute for Advanced Studies FIAS, Germany
¹⁶Institute of Physics, Bhubaneswar 751005, India
¹⁷Indian Institute of Technology, Mumbai, India
¹⁸Indiana University, Bloomington, Indiana 47408, USA
¹⁹Alikhanov Institute for Theoretical and Experimental Physics, Moscow, Russia
²⁰University of Jammu, Jammu 180001, India
²¹Joint Institute for Nuclear Research, Dubna, 141 980, Russia
²²Kent State University, Kent, Ohio 44242, USA
²³University of Kentucky, Lexington, Kentucky, 40506-0055, USA
²⁴Korea Institute of Science and Technology Information, Daejeon, Korea
²⁵Institute of Modern Physics, Lanzhou, China
²⁶Lawrence Berkeley National Laboratory, Berkeley, California 94720, USA
²⁷Massachusetts Institute of Technology, Cambridge, Massachusetts 02139-4307, USA
²⁸Max-Planck-Institut für Physik, Munich, Germany
²⁹Michigan State University, East Lansing, Michigan 48824, USA
³⁰Moscow Engineering Physics Institute, Moscow Russia
³¹National Institute of Science Education and Research, Bhubaneswar 751005, India
³²Ohio State University, Columbus, Ohio 43210, USA
³³Old Dominion University, Norfolk, Virginia 23529, USA
³⁴Institute of Nuclear Physics PAN, Cracow, Poland
³⁵Panjab University, Chandigarh 160014, India
³⁶Pennsylvania State University, University Park, Pennsylvania 16802, USA
³⁷Institute of High Energy Physics, Protvino, Russia
³⁸Purdue University, West Lafayette, Indiana 47907, USA
³⁹Pusan National University, Pusan, Republic of Korea
⁴⁰University of Rajasthan, Jaipur 302004, India
⁴¹Rice University, Houston, Texas 77251, USA
⁴²University of Science and Technology of China, Hefei 230026, China
⁴³Shandong University, Jinan, Shandong 250100, China
⁴⁴Shanghai Institute of Applied Physics, Shanghai 201800, China
⁴⁵SUBATECH, Nantes, France
⁴⁶Temple University, Philadelphia, Pennsylvania 19122, USA
⁴⁷Texas A&M University, College Station, Texas 77843, USA
⁴⁸University of Texas, Austin, Texas 78712, USA
⁴⁹University of Houston, Houston, Texas 77204, USA
⁵⁰Tsinghua University, Beijing 100084, China
⁵¹United States Naval Academy, Annapolis, Maryland, 21402, USA
⁵²Valparaiso University, Valparaiso, Indiana 46383, USA
⁵³Variable Energy Cyclotron Centre, Kolkata 700064, India
⁵⁴Warsaw University of Technology, Warsaw, Poland
⁵⁵University of Washington, Seattle, Washington 98195, USA
⁵⁶Wayne State University, Detroit, Michigan 48201, USA
⁵⁷Yale University, New Haven, Connecticut 06520, USA
⁵⁸University of Zagreb, Zagreb, HR-10002, Croatia

Local parity-odd domains are theorized to form inside the Quark-Gluon-Plasma (QGP) produced in high energy heavy ion collisions, and to manifest themselves as charge separation along the magnetic field via the chiral magnetic effect. The experimental observation of such a charge separation has been reported by STAR for Au+Au collisions at center of mass energy ($\sqrt{s_{NN}}$) of 200 GeV.

We present the evolution of the charge correlations for Au+Au collisions at midrapidity for $\sqrt{s_{NN}} = 7.7, 11.5, 19.6, 27, 39$ and 62.4 GeV. The signal gradually reduces with decreased beam energy, and tends to vanish around 7.7 GeV. This indicates the dominance of hadronic interactions over partonic interactions at lower collision energies.



PACS numbers: 25.75.-q

The strong interaction is parity even at vanishing temperature and isospin density [1], but parity could be violated locally in microscopic domains in QCD at finite temperature as a consequence of topologically non-trivial configurations of gauge fields [2, 3]. The Relativistic Heavy Ion Collider (RHIC) provide a good opportunity to study such parity-odd (\mathcal{P} -odd) domains, where the local imbalance of chirality results from the interplay of these topological configurations with the hot, dense and deconfined Quark-Gluon-Plasma (QGP) created in the heavy ion collisions.

The \mathcal{P} -odd domains can be manifested via the chiral magnetic effect (CME). In heavy ion collisions, energetic protons (mostly spectators) produce a strong magnetic field peaking around $eB \approx m_\pi^2$ [4], illustrated in Fig. 1. The strong magnetic field, coupled with the chiral asymmetry in the \mathcal{P} -odd domains, induces the electric charge separation along the direction of the magnetic field [4–9]. Based on data from STAR [10–12] and PHENIX [13, 14] Collaborations at RHIC and ALICE [15] at LHC, pertinent charge-separation fluctuations were experimentally observed. The interpretation of this as CME is still under intense discussion, see e.g. [16, 17] and references therein.

Experimentally the fluctuations of charge separation are measured along the axis of the magnetic field, perpendicular to the reaction plane (containing the impact parameter and the beam momenta), with a three-point correlator, $\gamma \equiv \langle \cos(\phi_1 + \phi_2 - 2\Psi_{RP}) \rangle$ [18]. Here ϕ and Ψ_{RP} denote the azimuthal angles of a particle and the reaction plane, respectively. In practice, we approximate the reaction plane with the “event plane” (Ψ_{EP}) reconstructed with measured particles, and then correct the measurement for the finite event plane resolution [10–12].

This Letter reports the measurements of γ for charged particles produced in Au+Au collisions of 8M events at 62.4 GeV (2005), 100M at 39 GeV (2010), 46M at 27 GeV (2011), 20M at 19.6 GeV (2011), 10M at 11.5 GeV (2010) and 4M at 7.7 GeV (2010). Events selected with a minimum bias trigger have been sorted into centrality classes based on uncorrected charged particle multiplicity at midrapidity. Charged particle tracks in this analysis were reconstructed in the STAR Time Projection Chamber (TPC) [19], within a pseudorapidity range of $|\eta| < 1$ and a transverse momentum range of $0.15 < p_T < 2$ GeV/c. The centrality definition and track quality cuts are the same as in Ref. [20], unless otherwise specified. Only events within 40 cm of the center of the detector along the beam direction were selected for data sets at $\sqrt{s_{NN}} = 19.6 - 62.4$ GeV. This cut was 50 (70) cm for

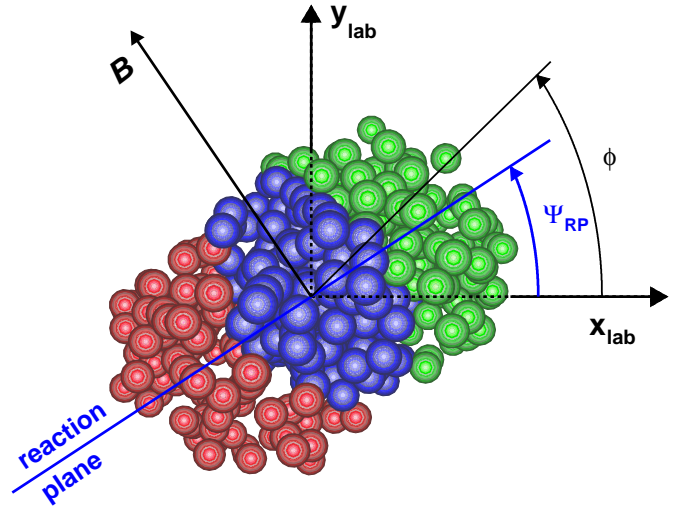


FIG. 1: (Color online) Schematic depiction of the transverse plane in a collision of two heavy ions (the left one emerging from and the right one going into the page). Particles are produced out of the overlap region (blue-colored nucleons). The azimuthal angles of the reaction plane and a produced particle used in the three-point correlator, γ , are depicted here.

11.5 (7.7) GeV collisions. To suppress events from collisions with the beam pipe (radius 3.95 cm), those with the radial position of the reconstructed primary vertex within 2 cm was analyzed. The distance of the closest approach to the primary vertex (DCA) < 2 cm was also applied to reduce the number of weak decay tracks or secondary interactions. The experimental observables involved in the analysis have been corrected for the particle track reconstruction efficiency.

In an event, charge separation along the magnetic field (perpendicular to the reaction plane) may be described phenomenologically by sine terms in the Fourier decomposition of the charged particle azimuthal distribution,

$$\frac{dN_{\pm}}{d\phi} \propto 1 + 2v_1 \cos(\Delta\phi) + 2a_{\pm} \sin(\Delta\phi) + 2v_2 \cos(2\Delta\phi) + \dots \quad (1)$$

where $\Delta\phi = \phi - \Psi_{RP}$. Conventionally v_1 is called “directed flow” and v_2 “elliptic flow”, and they describe the collective motion of the produced particles [21]. The parameter, $a_- = -a_+$, quantifies the \mathcal{P} -violating effect. The predicted spontaneous parity violation implies that the signs of a_+ and a_- vary from event to event, leading to $\langle a_+ \rangle = \langle a_- \rangle = 0$. In the ex-

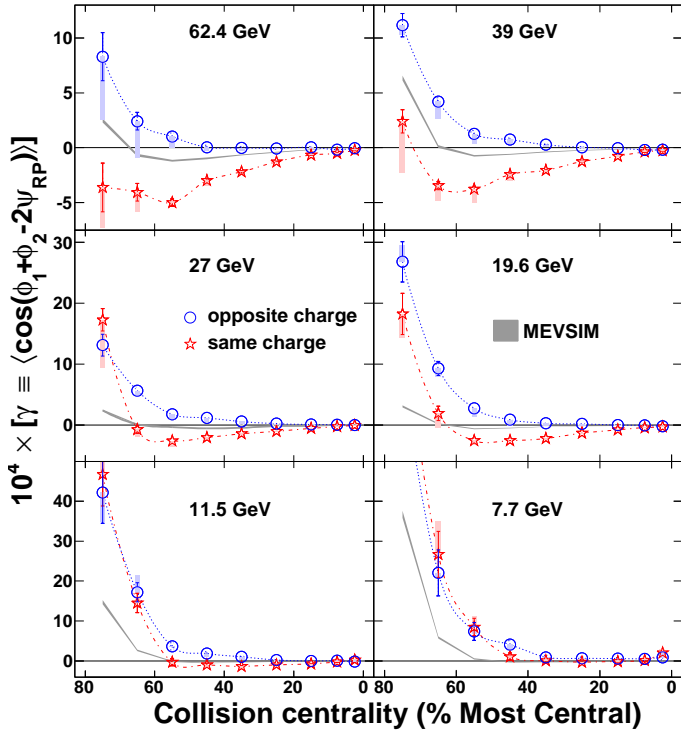


FIG. 2: (Color online) The three-point correlator, γ , as a function of centrality for Au+Au collisions at 7.7–62.4 GeV. Note that the vertical scales are different for different rows. The filled boxes represent one type of systematic uncertainties, starting from the central values and ending with the results with the extra conditions of $\Delta p_T > 0.15$ GeV/c and $\Delta \eta > 0.15$. These conditions were to suppress HBT+Coulomb effects (as discussed in the text).

pansion of the correlator, $\gamma = \langle \cos(\Delta\phi_1) \cos(\Delta\phi_2) - \sin(\Delta\phi_1) \sin(\Delta\phi_2) \rangle - \langle a_{\pm} a_{\pm} \rangle$, which may be non-zero when accumulated over particle pairs of separate charge combinations. The first term ($\langle \cos(\Delta\phi_1) \cos(\Delta\phi_2) \rangle$) in the expansion provides a baseline unrelated to the magnetic field.

The reaction plane of a heavy-ion collision is not known a priori, and in practice it is approximated with the event plane reconstructed from particle azimuthal distributions [21]. In this analysis, we exploited the large elliptic flow of charged hadrons produced at mid-rapidity to construct the event plane angle:

$$\Psi_{EP} = \frac{1}{2} \tan^{-1} \left[\frac{\sum \omega_i \sin(2\phi_i)}{\sum \omega_i \cos(2\phi_i)} \right], \quad (2)$$

where ω_i is a weight for each particle i in the sum [21]. The weight was chosen to be the p_T of the particle itself, and only particles with $p_T < 2$ GeV/c were used. Although the STAR TPC has good azimuthal symmetry, small acceptance effects in the calculation of the event plane azimuth were removed by the method of shifting [22]. The observed correlations were corrected for

the event plane resolution, estimated with the correlation between two random sub-events (details in Ref. [21]).

The event plane thus obtained from the produced particles is also called “the participant plane” since it is subject to the event-by-event fluctuations of the initial participant nucleons [23]. A better approximation to the reaction plane could be obtained from the spectator neutron distributions detected in the STAR zero degree calorimeters (ZDC-SMDs) [24]. This type of event plane utilizes the directed flow of spectator neutrons measured at very forward rapidity. As to the three-point correlator, measurements carried out with both types of event planes turned out to be consistent with each other [12]. Other systematic uncertainties were studied extensively in the previous publications on this subject [10, 11]. All were shown to be negligible compared with the uncertainty in determining the reaction plane. In this work, we only used the participant plane because the efficiency of ZDC-SMDs becomes very low for low beam energies.

Figure 2 presents the opposite-charge (γ_{OS}) and same-charge (γ_{SS}) correlators for Au+Au collisions at $\sqrt{s_{NN}} = 7.7 - 62.4$ GeV as a function of centrality (0 means the most central collisions). In most cases, the ordering of γ_{OS} and γ_{SS} is the same as in Au+Au (Pb+Pb) collisions at higher energies [10–12, 15], manifesting charge-separation fluctuations perpendicular to the reaction plane. As a systematic check, the charge combinations of ++ and -- are always found to be consistent with each other (not shown here). With decreased beam energy, both γ_{OS} and γ_{SS} tend to rise up in peripheral collisions. This feature seems to be charge independent, and can be explained by momentum conservation and elliptic flow [12]. Momentum conservation forces all produced particles, regardless of charge, to separate from each other, while elliptic flow works in the opposite sense. For peripheral collisions, the multiplicity (N) is small, and momentum conservation dominates. At lower beam energies, N also becomes smaller and hence higher values for γ_{OS} and γ_{SS} . For more central collisions where the multiplicity is large enough, this type of \mathcal{P} -even background can be estimated as $-v_2/N$ [12, 25]. In Fig. 2, we also show the model calculations of MEVSIM, a Monte Carlo event generator with the implementation of v_2 and momentum conservation, developed for STAR simulations [26]. The model results qualitatively describe the beam-energy dependency of the charge-independent background.

In view of the charge-independent background, the charge separation effect can be studied via the difference between γ_{OS} and γ_{SS} . The difference ($\gamma_{OS} - \gamma_{SS}$) remains positive for all centralities down to the beam energy ~ 19.6 GeV, and the magnitude decreases from peripheral to central collisions. Presumably this is partially owing to the reduced magnetic field and partially owing to the more pronounced dilution effect in more central collisions. The dilution of correlations occurs in

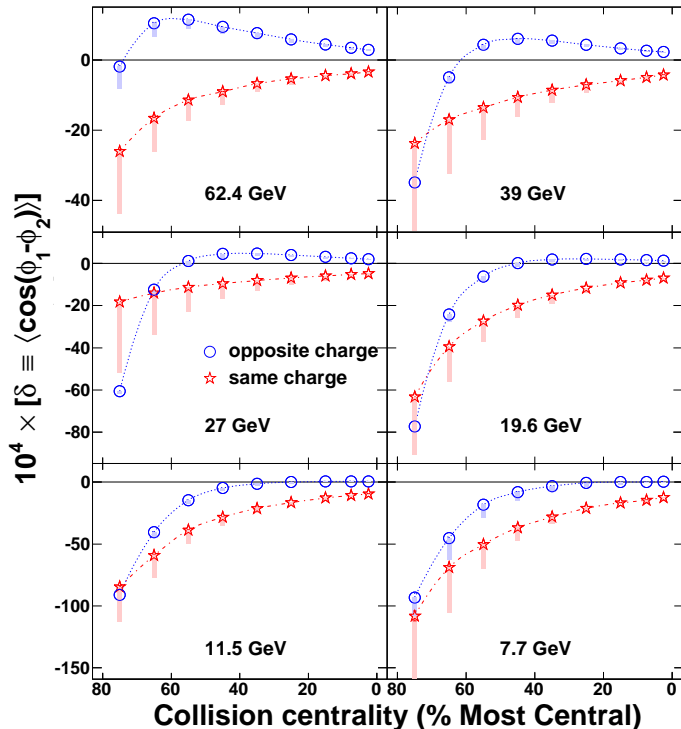


FIG. 3: (Color online) The two-particle correlation as a function of centrality for Au+Au collisions at 7.7–62.4 GeV. Note that the vertical scales are different for different rows. The filled boxes bear the same meaning as those in Fig 2.

the case of particle production from multiple sources [11]. The difference between γ_{OS} and γ_{SS} approaches zero in peripheral collisions at lower energies, especially at 7.7 GeV, which is understandable in the picture of CME as the formation of QGP becomes less likely in peripheral collisions at low beam energies [27].

The systematic uncertainties of $(\gamma_{OS} - \gamma_{SS})$ due to the analysis cuts, the track reconstruction efficiency and the event plane determination were estimated to be relative 10%, 5% and 10%, respectively. Overall, total systematic uncertainties are typically within 15%, except for the cases where $(\gamma_{OS} - \gamma_{SS})$ is close to zero. Another type of uncertainties is due to quantum interference (“HBT” effects) and final-state-interactions (Coulomb dominated) [12], which are most prominent for low relative momenta. To suppress the contributions from these effects, we applied the conditions of $\Delta p_T > 0.15$ GeV/c and $\Delta\eta > 0.15$ to the correlations, shown with filled boxes in Figs. 2, 3 and 4.

The interpretation of the γ results demands additional information on a two-particle correlation $\delta \equiv \langle \cos(\phi_1 - \phi_2) \rangle = \langle \cos(\Delta\phi_1)\cos(\Delta\phi_2) + \sin(\Delta\phi_1)\sin(\Delta\phi_2) \rangle$. The expansion of δ also contains the fluctuation term $\langle a_{\pm}a_{\pm} \rangle$. Figure 3 shows δ as a function of centrality for Au+Au collisions at 7.7 – 62.4 GeV. In most cases, δ_{OS} is above δ_{SS} , indicating an

overwhelming background over any possible CME effect. The background sources, if coupled with collective flow, will also contribute to γ . Taking this into account, one can express γ and δ in the following forms, where the unknown parameter κ , as argued in Ref. [28], is of the order of unity.

$$\gamma \equiv \langle \cos(\phi_1 + \phi_2 - 2\Psi_{RP}) \rangle = \kappa v_2 F - H \quad (3)$$

$$\delta \equiv \langle \cos(\phi_1 - \phi_2) \rangle = F + H, \quad (4)$$

where H and F are the CME and background contributions, respectively. In Ref. [28] $\kappa = 1$, but it could deviate from unity owing to the finite detector acceptance and other theoretical uncertainties. We can solve for H from Eqns. 3 and 4,

$$H^{\kappa} = (\kappa v_2 \delta - \gamma) / (1 + \kappa v_2). \quad (5)$$

Figure 4 shows $H_{SS} - H_{OS}$ as a function of beam energy for three centrality bins in Au+Au collisions. The default values (dotted curves) are from $H^{\kappa=1}$, and the solid (dash-dot) curves are obtained with $\kappa = 1.5$ ($\kappa = 2$). For comparison, the results for 10 – 60% Pb+Pb collisions at 2.76 TeV are also shown [15]. In the case $\kappa = 1$, $(H_{SS} - H_{OS})$ demonstrates a weak energy dependency above 19.6 GeV, and tends to diminish from 19.6 to 7.7 GeV. This may be explained by the probable domination of hadronic interactions over partonic ones at low beam energies. With increased κ , $(H_{SS} - H_{OS})$ decreases for all beam energies and may even totally disappear in some case (e.g. with $\kappa \sim 2$ in 10 – 30% collisions). A better theoretical estimate of κ in future will enable to extract a more conclusive result from Fig. 4 with interpolation or extrapolation of the data presented.

In summary, a three-point correlation between two charged particles and the reaction plane has been carried out for Au+Au collisions at $\sqrt{s_{NN}} = 7.7 - 62.4$ GeV. The general trend of separate correlations (γ_{OS} and γ_{SS}), as a function of centrality and beam energy can be qualitatively described by the model calculations of MEVSIM, indicating the contribution from the \mathcal{P} -even background due to momentum conservation and collective flow. The charge separation along the magnetic field studied via $(H_{SS} - H_{OS})$, shows a weak energy dependency down to 19.6 GeV and then vanishes at lower energies. This is consistent with the picture of a smaller probability for local parity violation and chiral magnetic effect when the hadronic phase plays an increased role with decreased energy. A more conclusive result can be obtained in future if we could increase the event statistics by ten times for the low energies and if we could reduce the uncertainty associated with determination of the value of κ .

We thank the RHIC Operations Group and RCF at BNL, the NERSC Center at LBNL, the KISTI Center in Korea and the Open Science Grid consortium for providing resources and support. This work was supported in part by the Offices of NP and HEP within the U.S.

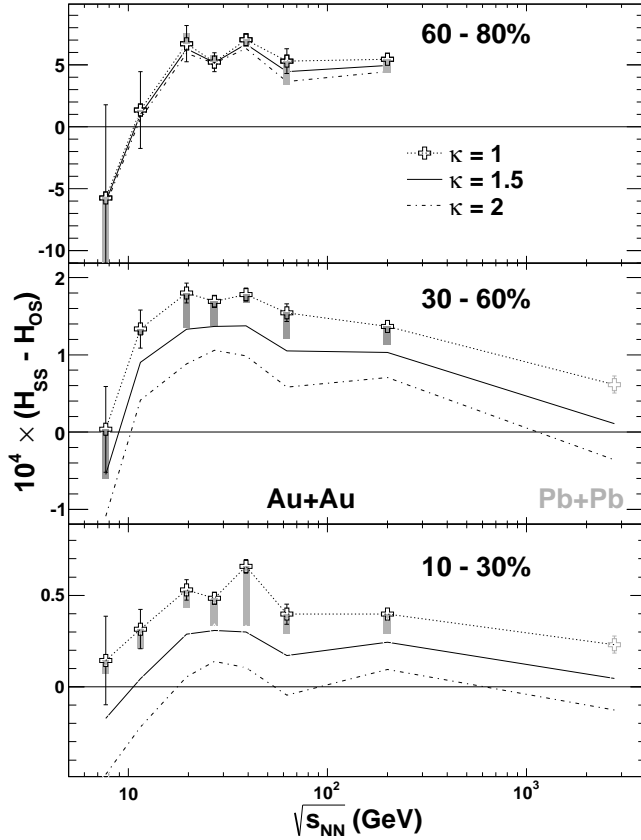


FIG. 4: (Color online) $H_{SS} - H_{OS}$, as a function of beam energy for three centrality bins in Au+Au collisions. The default values (dotted curves) are from $H^{\kappa=1}$, and the solid (dash-dot) curves are obtained with $\kappa = 1.5$ ($\kappa = 2$). For comparison, the results for Au+Au collisions at 200 GeV [11] and Pb+Pb collisions at 2.76 TeV [15] are also shown. The systematic errors of the STAR data (filled boxes) bear the same meaning as those in Fig. 2.

DOE Office of Science, the U.S. NSF, CNRS/IN2P3, FAPESP CNPq of Brazil, Ministry of Ed. and Sci. of the Russian Federation, NNSFC, CAS, MoST and MoE of China, the Korean Research Foundation, GA and MSMT of the Czech Republic, FIAS of Germany, DAE, DST, and CSIR of India, National Science Centre of Poland, National Research Foundation (NRF-2012004024), Ministry of Sci., Ed. and Sports of the Rep. of Croatia, and RosAtom of Russia.

-
- [1] C. Vafa and E. Whitten, Phys. Rev. Lett. **53**, 535 (1984).
 - [2] T. D. Lee, Phys. Rev. D **8**, 1226 (1973).
 - [3] T. D. Lee and G. C. Wick, Phys. Rev. D **9**, 2291 (1974).
 - [4] D. E. Kharzeev, L. D. McLerran and H. J. Warringa, Nucl. Phys. A **803**, 227 (2008).
 - [5] D. Kharzeev, Phys. Lett. B **633**, 260 (2006).
 - [6] D. Kharzeev and A. Zhitnitsky, Nucl. Phys. A **797**, 67 (2007).
 - [7] K. Fukushima, D. E. Kharzeev and H. J. Warringa, Phys. Rev. D **78**, 074033 (2008).
 - [8] D. E. Kharzeev, Annals Phys. **325**, 205 (2010).
 - [9] R. Gatto and M. Ruggieri, Phys. Rev. D **85**, 054013 (2012).
 - [10] B. I. Abelev *et al.* [STAR Collaboration], Phys. Rev. Lett. **103**, 251601 (2009).
 - [11] B. I. Abelev *et al.* [STAR Collaboration], Phys. Rev. C **81**, 054908 (2010).
 - [12] L. Adamczyk *et al.* [STAR Collaboration], Phys. Rev. C **88**, 064911 (2013).
 - [13] N. N. Ajitanand, S. Esumi, R. A. Lacey [PHENIX Collaboration], in: Proc. of the RBRC Workshops, vol. 96, 2010: "P- and CP-odd effects in hot and dense matter".
 - [14] N. N. Ajitanand, R. A. Lacey, A. Taranenko and J. M. Alexander, Phys. Rev. C **83** 011901, (2011).
 - [15] B. I. Abelev *et al.* [ALICE Collaboration], Phys. Rev. Lett. **110**, 021301 (2013).
 - [16] A. Bzdak, V. Koch and J. Liao, Phys. Rev. C **81**, 031901 (2010); Phys. Rev. C **82**, 054902 (2010).
 - [17] D. E. Kharzeev and D. T. Son, Phys. Rev. Lett. **106**, 062301 (2011).
 - [18] S. Voloshin, Phys. Rev. C **70**, 057901 (2004).
 - [19] M. Anderson *et al.*, Nucl. Instr. Meth. A **499**, 659 (2003).
 - [20] L. Adamczyk *et al.* [STAR Collaboration], Phys. Rev. C **86**, 54908 (2012).
 - [21] A. M. Poskanzer and S. A. Voloshin, Phys. Rev. C **58**, 1671 (1998).
 - [22] J. Barrette *et al.*, Phys. Rev. C **56**, 3254 (1997).
 - [23] J. -Y. Ollitrault, A. M. Poskanzer and S. A. Voloshin, Phys. Rev. C **80**, 014904 (2009).
 - [24] B. I. Abelev *et al.* [STAR Collaboration], Phys. Rev. Lett. **101**, 252301 (2008); and references therein.
 - [25] A. Bzdak, V. Koch and J. Liao, Phys. Rev. C **83**, 014905 (2011).
 - [26] R. L. Ray and R. S. Longacre, arXiv:nucl-ex/0008009 and private communication.
 - [27] V.A. Okorokov, Int. J. Mod. Phys. E **22**, 1350041 (2013).
 - [28] A. Bzdak, V. Koch and J. Liao, Lect. Notes Phys. **871**, 503 (2013).